Chemically Active Reduced Graphene Oxide with Tunable C/O Ratios

Owen C. Compton,[†,‡] Bonny Jain,[†] Dmitriy A. Dikin,[§] Ali Abouimrane,[‡] Khalil Amine,[‡] and SonBinh T. Nguyen[*,†,‡]

[†]Department of Chemistry, Northwestern University, 2145 Sheridan Road, Evanston, Illinois 60208-3133, United States, [‡]Materials Sciences and Engineering Division, Argonne National Laboratory, 9700 South Cass Avenue, Argonne, Illinois 60439, United States, and [§]Department of Mechanical Engineering, Northwestern University, 2145 Sheridan Road, Evanston, Illinois 60208-3133, United States

ABSTRACT Organic dispersions of graphene oxide can be thermally reduced in polar organic solvents under reflux conditions to afford electrically conductive, chemically active reduced graphene oxide (CARGO) with tunable C/O ratios, dependent on the boiling point of the solvent. The reductions are achieved after only 1 h of reflux, and the corresponding C/O ratios do not change upon further thermal treatment. Hydroxyl and carboxyl groups can be removed when the reflux is carried out above 155 °C, while epoxides are removable only when the temperature is higher than 200 °C. The increasing hydrophobic nature of CARGO, as its C/O ratio increases, improves the dispersibility of the nanosheets in a polystyrene matrix, in contrast to the aggregates formed with CARGO having lower C/O ratios. The excellent processability of the obtained CARGO dispersions is demonstrated *via* free-standing CARGO papers that exhibit tunable electrical conductivity/chemical activity and can be used as lithium-ion battery anodes with enhanced Coulombic efficiency.

KEYWORDS: graphene · graphene oxide · surface functionalization · thermal reduction · lithium-ion battery

Graphene nanosheets are atomically thick, two-dimensional platelets featuring carbon atoms in a honeycomb arrangement. These sp^2-hybridized sheets of carbon possess a host of desirable properties, including high mechanical stiffness (1 TPa),[1] good thermal conductivity (5000 W m^{-1} K^{-1}),[2] and excellent charge carrier mobility (250 000 cm^2 V^{-1} s^{-1}).[3] As such, graphene has been studied for use in a variety of applications that exploit these properties,[4,5] ranging from gas sensors[6] to lithium-ion battery electrodes.[7,8] The primary synthetic procedure for producing processable quantities of colloidal graphene (also called highly reduced graphene oxide, HRG)[9] entails the reduction of aqueous or organic dispersions of graphene oxide,[10] a highly oxidized derivative of graphene possessing various oxygen-containing functional groups (epoxy, hydroxyl, carbonyl, and carboxyl).[11−14] These groups, found on both the edge and basal plane of the nanosheets, introduce sp^3 defect sites to the nanosheets, distorting the intrinsic conjugated π system and lowering overall strength and conductivity.[15] Nevertheless, the reactivity of these groups makes graphene oxide nanosheets highly attractive as building blocks for a wide range of macroscopic structures, as they can be readily modified with a variety of "surfactants".[16,17]

Current reduction methods for producing colloidal graphene from graphene oxide typically afford nanosheets with high C/O ratios (~10)[10] that exhibit good electrical conductivity, but are effectively inactive for chemical functionalization due to the low density of reactive groups remaining on the sheet surface. Although the resulting HRG can be used for electronic applications,[9,18] the inability to access functionalized graphene-based materials hinders the development of other applications that do not solely rely on good conductivity. For example, functionalized biocompatible graphene[4] may see use in the encapsulation of enzymes[19] or as a template for DNA attachment.[20] Herein, we present a facile technique for the production of colloidal dispersions of chemically active reduced graphene oxide (CARGO) with tunable C/O ratios (from ~3 to ~5) between that of graphene oxide (~2) and HRG (~10). The versatility of these processable dispersions is demonstrated by their fabrication into free-standing papers that exhibit good electrical conductivity while retaining chemical activity for surface functionalization in a well-controlled, tunable fashion. We additionally demonstrate the advantage of isocyanate-functionalized CARGO over unfunctionalized CARGO as a binder-free lithium-ion battery anode with enhanced charge retention and reversible capacity.

RESULTS AND DISCUSSION

Selection of Solvents for CARGO Synthesis. The majority of methods for the preparation of graphene from oxidized derivatives rely

* Address correspondence to stn@northwestern.edu.

Received for review November 12, 2010 and accepted April 7, 2011.

Published online April 07, 2011
10.1021/nn1030725

upon either harsh thermal or chemical reductive conditions. For example, functionalized graphene sheets in powder form can be collected after exposing graphite oxide (GO) powder to extremely high temperatures (>1000 °C).[21,22] However, this thermal reduction technique yields only solid aggregates that are not easily redispersed in solvent, limiting their further processing into functional materials like polymer nanocomposites[5] or paper-like films.[23] Reduction of aqueous or organic graphene oxide dispersions can also be achieved in solution by treatment with reducing agents, such as hydrazine,[24] sodium borohydride,[25] or vitamin C.[26] Unfortunately, this approach usually affords only aggregates unless surface-stabilizing agents are employed,[27,28] whose presence can significantly lower conductivity[15] and limit further chemical functionalization.

To date, few studies[9,23,29,30] have reported the successful reduction of graphene oxide dispersions to afford colloidal graphene in the absence of steric- or charge-stabilizers. In addition, these works have all focused on producing highly reduced, and therefore chemically inactive, graphene with C/O ratios near 10 for electronic applications. To expand the scope of functionalizable graphene materials, we have prepared colloidal dispersions of CARGO in a variety of organic solvents *via* a "low-temperature" thermal reduction. This thermal-treatment approach was motivated by the observation of a significant mass loss feature initiating near 150 °C in the thermogravimetric analysis (TGA) profile of graphene oxide (Figure S1A in Supporting Information (SI)), which has been attributed to a major loss of oxygen-containing functionalities.[31] While thermal treatment has previously been applied to prepare graphene from GO powder,[21,22] the low-temperature "location" of the aforementioned TGA feature suggests that the high temperatures applied in those earlier studies (>1000 °C) were excessive for producing processable colloidal dispersions. Indeed, Dai and co-workers have observed that solvothermal reduction of GO can be achieved in DMF at only 180 °C.[32] The groups of Ruoff[30] and Kaner[33] have also recently demonstrated that exposing dispersions of graphene oxide to temperatures above 150 °C can produce reduced graphene oxide with C/O ratios between 5.2 and 8.3.

To achieve thermal reduction of graphene oxide in solution without aggregate formation, we hypothesize that the dispersing medium must meet two conditions: (1) have a boiling point (bp) above 150 °C, the initiation point of the mass loss feature in the TGA profile of graphene oxide (see preceding paragraph) and (2) be able to disperse both graphene oxide and CARGO. As such, we selected *N,N*-dimethylformamide (DMF, bp = 153 °C), dimethyl sulfoxide (DMSO, bp = 189 °C), and *N*-methylpyrrolidone (NMP, bp = 204 °C) as candidates in our study. We were pleased to observe the conversion

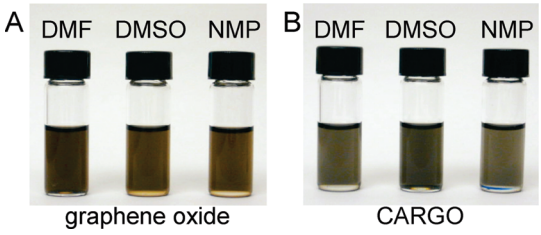

Figure 1. Digital images of graphene oxide (A) and CARGO (B) dispersions in various organic solvents (concentration ≈ 0.05 mg mL^{-1}), demonstrating the shift in color from brown to black after reduction.

of graphene oxide dispersions from brown to black (*cf.* Figure 1A,B) in each of these three solvents after ~15 min of reflux, indicating reduction to CARGO. Small flocculates that formed along the air/solvent boundary of the dispersions in DMF and NMP were readily redispersed by brief sonication (30 s) of the cooled solutions.

As prepared, the CARGO dispersions have remained stable, with no formation of aggregates, in all three solvents for over seven months, up to the submission of this manuscript. That highly stable CARGO can be obtained simply by thermal reduction in DMSO and NMP is remarkable, as hydrazine reduction of graphene oxide in those solvents has been observed to produce only aggregates (Figure S2 in SI),[9] likely a result of poor interaction between the highly reduced, nonpolar graphene surface with these polar solvents.

Effect of Reflux Temperature and Length on C/O Ratio. Given the wide variety of oxygen-containing functional groups on graphene oxide, along with the different mechanisms involved in their thermal reduction,[34] we hypothesized that the nanosheet surface functionality can be controlled *via* "annealing" temperature and length. To this end, we monitored the C/O ratios (Table 1) of our graphene oxide before and after reflux in DMF, DMSO, and NMP for 1 and 12 h. A direct dependence was observed between the C/O ratio of the CARGO (*i.e.*, the graphene oxide post-reflux) and the boiling point of the solvent, with 1 h reflux in DMF, DMSO, and NMP increasing the C/O ratio of CARGO to 2.7, 4.0, and 4.4, respectively, from 1.7 ± 0.1 in the parent graphene oxide. While seemingly *small* in scale, these increased ratios represent *large* decreases in oxygen content, from ~40% to ~60%, on the reduced CARGO surface. That oxygen loss increases with increasing reflux temperatures is intuitively obvious given our thermal-reduction hypothesis.[35] As our results demonstrate a strong relationship between the extent of reduction and solvent boiling point (Figure S3 in SI), refluxing graphene oxide in organic solvents with different boiling points offers a facile means by which the C/O ratio of CARGO can be tuned between that of graphene oxide (C/O ratio ~2) and HRG (C/O ratio ~10).

TABLE 1. Composition and Characterization of CARGO Prepared in Various Organic Solvents

		C/O ratio[a]					
solvent	annealing temp (°C)	initial	1 h reflux	12 h reflux	intersheet spacing (Å)	conductivity (S m^{-1})[b,c]	thickness (μm)[b]
no reflux	N/A	1.7 ± 0.1[d]	N/A	N/A	9.7 ± 0.5[d]	$<10^{-3}$	10.2
DMF	153	1.6	2.7	2.8	3.69[b]	12 ± 2	11.5
DMSO	153	1.8	3.1	3.3	3.38	9 ± 3	6.8
DMSO	189	1.8	4.0	4.0	3.63[b]	52 ± 9	9.4
NMP	153	1.8	3.1	3.2	3.75	15 ± 3	16.2
NMP	189	1.8	3.8	3.9	3.62	9 ± 4	4.1
NMP	204	1.8	4.4	4.4	3.61[b]	48 ± 7	7.3

[a] C/O ratios are calculated based on the amount of native carbon present in the nanosheets and does not include the carbon from solvent (see sample calculation in the SI). [b] Values reported are those obtained from paper samples made from the corresponding colloidal materials [c] Standard deviations are calculated based upon variations of ±1 μm in paper thickness, as measured by scanning electron microscopy (Figure S7 in SI), and uncertainties in the spacing between the electrical voltage probes on the sample. [d] Values are averaged from all unreduced graphene oxide paper samples

Surprisingly, extending the reflux period from 1 to 12 h increased the C/O ratio an average of only 2% for all three solvents (Table 1). This suggests that 1 h of thermal treatment at a temperature above 150 °C is sufficient to remove the oxygen-containing functional groups that are labile at that temperature from graphene oxide. The higher the reflux temperature of the solvent, the easier it is to remove the more resilient groups (epoxy and carbonyl) from the nanosheet surface (see Characterization of CARGO Papers section). Such an effect is supported by comparing the TGA profiles (Figure 2A, see also the corresponding first-derivative plots in Figure 2B) of thermally reduced CARGO samples where clear mass loss features can be observed near the boiling temperature of the respective solvent in which each sample was refluxed. In particular, CARGO samples prepared from DMF, DMSO, and NMP lose 5.6, 3.1, and 1.6% of their initial masses, respectively, in the 150−200 °C region. This trend illustrates that the higher reflux temperatures of NMP (bp = 204 °C) and DMSO (bp = 189 °C) remove more oxygen-containing functionalities from the nanosheet compared to DMF (bp = 153 °C).

Independence of C/O Ratio on Solvent Type. While the aforementioned strong correspondence between the reflux temperature at which the CARGO sample was prepared and its extent of reduction suggests a facile means for tuning the C/O ratio in CARGO, relying upon the solvent boiling temperatures would limit the degree of fine-tuning within a large range of possible ratios. A potential additional complication is the interaction between graphene oxide and certain solvents such as DMF, which has been observed to affect the efficiency of graphene oxide reduction.[36] Thus, to demonstrate the flexibility of thermal reduction and eliminate any concerns over solvent effects, CARGO was prepared by heating graphene oxide in NMP at the boiling points of DMF or DMSO (189 °C) and in DMSO at the boiling point of DMF (153 °C). As expected for a solvent-independent reduction mechanism, the C/O ratios achieved at each temperature, regardless of solvent and reflux time, are consistently within 15% of each other (Table 1). Such high consistency confirms that thermal reduction from graphene oxide to CARGO is only dependent upon temperature, with the identity of the intercalated solvent being the only difference among CARGO samples prepared in different solvents. We note that such residual solvent molecules may affect certain physical properties of these materials, such as conductivity (see Properties of CARGO Papers section).

Dispersibility of CARGO in a Polystyrene Matrix as a Function of C/O Ratio. As the C/O ratio of our CARGO nanosheets is increased, the hydrophobicity of the sheets increases concurrently. Variance in this surface property can be best evaluated by monitoring the dispersibility of the nanosheets in a hydrophobic polymer matrix. For this purpose, 1 wt % of CARGO nanosheets prepared in DMF, DMSO, and NMP were solution-blended into a polystyrene matrix, and the resulting nanocomposites were precipitated and hot-pressed into thin films. The scanning electron microscope (SEM) images of these thin films revealed significant variation in the nanosheet dispersion within the hydrophobic polystyrene matrix. The most hydrophilic CARGO nanosheets, those prepared in DMF with the lowest C/O ratio, form large aggregates that span micrometers within the nanocomposite (Figure 3D). With increasing nanosheet hydrophobicity, as shown by its increased C/O ratio, the CARGO prepared in DMSO forms much smaller aggregates inside the polymer phase (Figure 3E). The most hydrophobic CARGO sample, that prepared in NMP, does not aggregate to any significant degree inside the polystyrene matrix. Instead, its nanosheets are largely dispersed within the polymer (Figure 3F). Such vast differences in nanosheet dispersivity demonstrate an important utility for tuning the C/O ratio of CARGO: the dispersibility of a CARGO nanofiller can be adjusted to achieve different types of graphene−polymer nanocomposites.

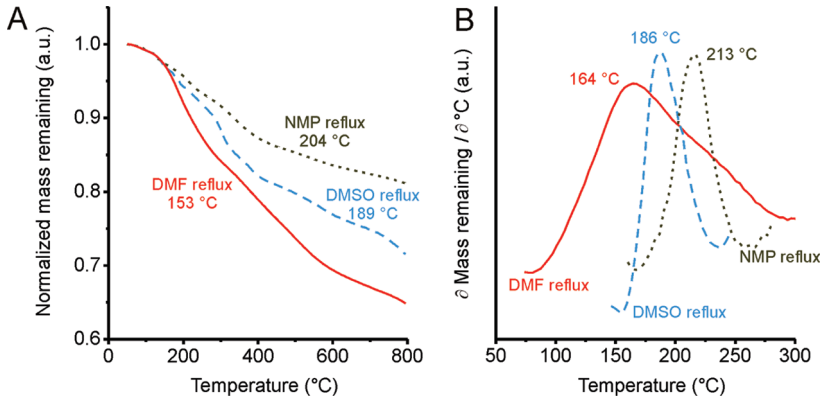

Figure 2. (A) TGA profiles of CARGO samples prepared by refluxing in DMF (red), DMSO (blue), and NMP (gray). (B) Scaled first-derivative plots of the TGA curves in (A) with temperatures denoted at which the mass loss feature initiates for each curve. The peak in each curve illustrates that the mass-loss feature in each profile occurs near the temperature at which the sample was refluxed.

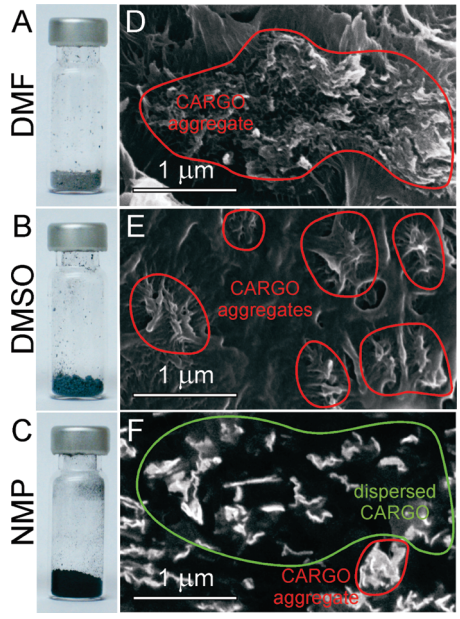

Figure 3. (A, B, and C) Digital images of CARGO–polystyrene nanocomposite powders containing 1 wt % of each of the three types of CARGO as nanofiller, with samples containing the more-reduced CARGO (*i.e.*, the CARGO with higher C/O ratios) showing progressively darker colors. The solvents used to prepare these CARGO nanosheets are noted on the left-hand side of each image. (D, E, and F) Corresponding SEM images of thin films of the nanocomposites after hot-pressing, demonstrating the improved dispersivity of CARGO nanofiller with increasing C/O ratio inside the polystyrene matrix. Regions containing aggregates of CARGO nanosheets are highlighted in red, while those containing dispersed CARGO are circled in green.

An additional benefit for having a tunable C/O ratio in CARGO nanofiller is the increased optical opacity of CARGO–polystyrene nanocomposite thin films as the C/O ratio increases. Prior to being hot-pressed into thin films, our CARGO–polystyrene (1 wt % of CARGO) nanocomposite powders ranged in color from light gray to black, with the one containing the more-reduced CARGO (*i.e.*, having higher C/O ratios) having darker colors (Figures 3A–C). This is expected given the increases in the proportions of sp^2 carbon from the growing graphene-like regions as the C/O ratio is increased in the CARGO nanosheet. This difference in color is more pronounced visually when nanocomposite powders containing less nanofiller (0.025 wt % of CARGO) were hot-pressed into ~0.25-mm-thick films (Figure S4A in SI). The resulting films exhibited increasing opacity as C/O ratio increased (Figure S4B in SI), likely a combination of the aforementioned increase in the number of sp^2 carbons and poor dispersion of the more hydrophobic nanofiller. This increased opacity could be used to decrease light transmission through the composite film, a highly desirable property for packaging materials.[37]

Characterization of CARGO Papers. While analysis of dried CARGO, in the form of a free-standing paper (see Properties of CARGO Papers section below), using X-ray photoelectron spectroscopy (XPS) can provide a means to identify which functional groups are being removed from the graphene oxide surface during reflux (Figure 4), quantitative interpretation of the XPS spectra of the CARGO samples is difficult due to cluttering signals from residual solvent.[38] Such signals appear as peaks that overlap with the graphene oxide C1s XPS signal from our dried CARGO samples: C–N and C(O-)–N components (~286.4 and ~287.5 eV, respectively-)[39] can be observed from residual DMF and NMP, along with C–S bonds (~285.3 eV)[40] from DMSO. Despite these issues, comparison of the C1s XPS spectra of graphene oxide before and after reflux reveals a clear strengthening and narrowing of the graphitic C–C signal (284.5 eV) in all solvents after reflux. Concurrently, a weakening of the signals for hydroxyl (C–OH, ~285.6 eV) and carboxyl (C(O)–OH, ~289.4 eV) groups after reflux in all solvents corresponds well with previous observations of hydroxyl and carboxyl loss in GO that was thermally annealed at 200 °C for only 2 h.[31] Signals for carbonyl groups (~287.8 eV) remain unaffected by reflux temperature, indicating that these

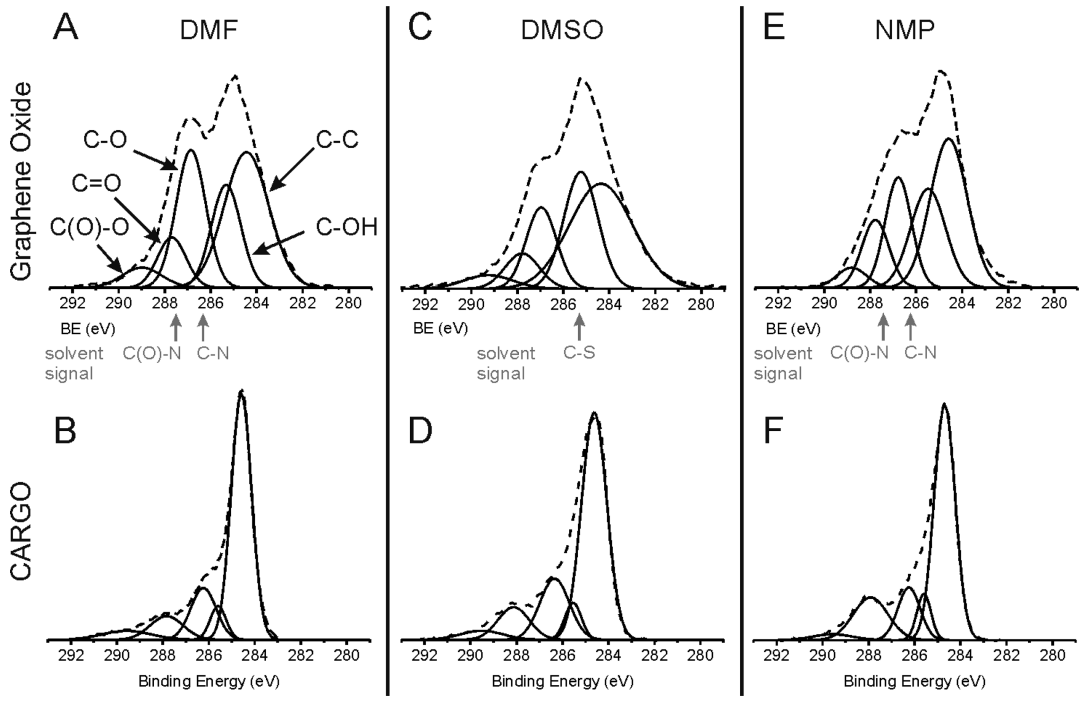

Figure 4. Deconvoluted XPS spectra of the C1s region of graphene oxide (A, C, and E) and CARGO (B, D, and F) samples prepared *via* refluxing in DMF, DMSO, and NMP, as denoted at the top of each column. The loss of oxygen-containing functionalities from graphene oxide (top row) to CARGO (bottom row) after reflux is evident. The labeling of the specific groups (from left to right: carboxyl, carbonyl, epoxy, hydroxyl, and graphite) in the upper left panel is consistent throughout all spectra. The locations of signal that would originate from residual solvent in each sample are indicated in light gray below the spectra in the "Graphene Oxide" row.

groups are stable on the CARGO surface during thermal treatment. Indeed, the remarkable resilience of carbonyl groups on GO and graphene oxide during annealing has been theoretically predicted in multiple studies.[34,41]

Interestingly, the signal for epoxy groups (~286.6 eV) in the NMP-refluxed sample is weaker than those in the DMF- and DMSO-refluxed ones, suggesting that the higher NMP reflux temperature may have removed some of the more strained epoxide groups.[42] Despite the aforementioned residual solvent signals, the loss of epoxide after reflux in NMP can be quantified from this data by integrating the areas beneath the individual deconvoluted XPS signals and comparing the ratio between the areas for residual epoxide (E_A) and carbonyl (C_A) groups on the CARGO surface. The aforementioned stability of the carbonyl groups keeps their concentration relatively constant in all solvents, making them the only suitable reference signal in the XPS spectrum, since all other peaks fluctuate after reduction. For those CARGO samples refluxed in DMF and DMSO, the E_A/C_A ratio is 1.69 and 1.77, respectively. However, reflux in NMP drastically decreases this ratio to 0.78, demonstrating that epoxide loss occurs most significantly at temperatures above 200 °C. We note that cooperative variation in C1s XPS signal, where loss of oxygen groups weakens the signals from the carbons bearing these groups while concurrently strengthens the graphitic signal from the carbons without oxygen, serves to artificially increase the apparent reduction of these materials in the spectra for CARGO samples.

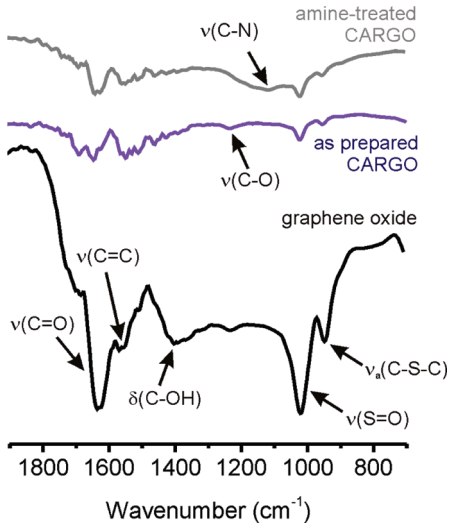

Figure 5. FT-IR spectra of graphene oxide and CARGO paper samples before and after hexylamine functionalization, demonstrating the significant reduction in oxygen-containing functionality signal in comparison to graphene oxide. All samples were prepared in DMSO, which contributes signal for the labeled peaks of ν(S═O) and ν_a(C—S—C). The reduction in signal-to-noise ratio when graphene oxide (bottom spectrum) is converted to CARGO (top spectra) is commonly seen in the literature,[26,36] presumably due to increased absorption and scattering upon reduction.

Qualitatively, the loss of oxygen-containing functional groups after thermal treatment is most apparent when comparing the Fourier-transform infrared (FT-IR)

spectra of the CARGO samples against those of their graphene oxide precursors (Figure 5 and Figure S5 in SI). Indeed, the infrared spectra of GO has been found to be extremely sensitive to the C/O ratio, where minor decreases in oxygen content (~20%) lower IR absorption by roughly 50%.[14] Prior to thermal treatment, strong signals are present in the FT-IR spectra of all graphene oxide samples for epoxy (υ(C−O) ≈ 1240 cm^{-1}), hydroxyl (δ(C−OH) ≈ 1400 cm^{-1}), carbonyl (υ(C═O) ≈ 1630 cm^{-1}), and carboxyl (same as carbonyl) functional groups.[31,39] After reflux, spectra for CARGO samples prepared from all solvents exhibit no signal for hydroxyl groups, while carbonyl signal from C═O bonds remains relatively strong. We note that the IR stretch for epoxy functionalities is still present in the spectra for DMF- and DMSO-prepared CARGO (Figures S5A and 5, respectively); however, it cannot be readily recognized in the spectrum of CARGO prepared from NMP (Figure S5B in SI). Given the indiscriminate, low-resolution nature of FT-IR spectra for heterogeneous powder samples, where one absorption band (C═O) can represent multiple functional groups (carbonyl and carboxyl), quantitative analysis of functional group concentration cannot be obtained from this data with any level of confidence.

Properties of CARGO Papers. The processability of colloidal CARGO in all three reaction solvents was demonstrated by their use in the fabrication of free-standing papers *via* vacuum-assisted filtration.[4,9] Given the decreased number of oxygen-containing functional groups on the CARGO surface, these papers are expected to exhibit interlayer spacing similar to that in pristine graphite (3.35 Å). Indeed, the X-ray diffraction (XRD) patterns for thermally reduced, air-dried CARGO papers prepared from DMF, DMSO, and NMP all contain well-defined peaks with spacing values of 3.64, 3.71, and 3.63 Å, respectively (Figure 6 and Figure S6 in SI). These values are shifted significantly from those of unreduced graphene oxide papers deposited from each solvent, which exhibit corresponding spacing values of 9.64, 9.25, and 10.22 Å, (Figure 6 and Figure S6 in SI). These ~6 Å shifts to smaller intersheet spacings in the CARGO paper structures should be primarily attributed to the loss of oxygen-containing functional groups during reflux, and are comparable to a previously observed shift for a hydrazine-reduced, assembled graphene oxide paper with a similar C/O ratio (near 5).[39] Given the lower C/O ratios of our CARGO papers, another contributing factor to this drastic shift may be a decrease in the amount of intercalated solvent within the paper structure due to increased hydrophobicity (see Dispersibility of CARGO in a Polystyrene Matrix section above). Indeed, the effect of solvent on interlayer spacing has been thoroughly explored for GO, where a hydrated sample exhibited much larger spacing (11 Å) than its completely anhydrous counterpart (7 Å).[43] The broad, low-

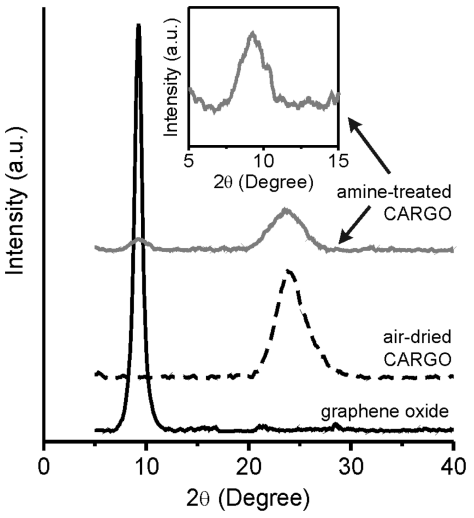

Figure 6. XRD patterns for papers of graphene oxide and CARGO, demonstrating the significant shift in intergallery spacing after thermal reduction. The pattern for hexylamine-treated CARGO paper exhibits a graphene peak near $2\theta = 24°$ and an additional peak near $2\theta = 9°$, indicating the presence of amine between adjacent sheets in the CARGO paper structure. Inset: Magnified plot of the diffraction peak near $2\theta = 9°$ for hexylamine-treated CARGO.

intensity diffraction peaks of the CARGO papers are not surprising, considering that air-dried graphene paper comprising hydrazine-reduced[4] or thermally reduced nanosheets[33] (C/O ratios of ~8 and ~5, respectively) exhibit similar patterns, both with intersheet spacings near 3.5 Å.

In-line, four-point-probe conductivity measurements of our CARGO samples, as self-supporting papers, indicated that they are much more electrically conductive (~50 S m^{-1}, Table 1) than graphene oxide papers (<10^{-3} S m^{-1}, Table 1), further confirming their graphene-like properties. The conductivities for these papers, were found to range from a low of 12 ± 2 S m^{-1} for the DMF-refluxed sample to a high of 52 ± 9 S m^{-1} for the DMSO-prepared one. While the supposedly more-reduced CARGO sample prepared from NMP exhibited slightly lower electrical conductivity (48 ± 7 S m^{-1}) than the DMSO-prepared sample, these values are within experimental error. That these conductivities are somewhat lower than those for non-annealed HRG papers (up to ~7000 S m^{-1})[4] can be attributed to the residual oxygen-containing functional groups on the surface of the CARGO sheets, which are localized on sp^3-hybridized carbons and limit the electrical conductivity of the paper samples. In addition, any small amounts of residual solvent or moisture trapped within the gallery of the CARGO paper would also reduce conductivity. The presence of solvent and/or moisture was unavoidable in our CARGO papers, as additional heat treatment to remove these adventitious species would further reduce the CARGO nanosheets and decrease the level of functional groups present in the paper. Solvent effect is most evident when comparing conductivity values for samples

prepared in the same solvent but at different temperatures (Table 1), where no correlation exists between C/O ratio and conductivity.

Temperature-dependent conductivity measurements (Figure S8A in SI) reveal a semiconducting-type behavior for CARGO samples prepared from all solvents, with the NMP- and DMSO-prepared materials closely mirroring each other, as expected from the aforementioned measurements at room temperature. Their current−voltage characteristics at low bias voltages (+1 to −1 V) are linear (Ohmic) and symmetric as current density approaches 10^5 A m^{-2} (Figure S8B in SI), while at higher bias voltages the conduction increases. In general, this behavior is similar to that reported for individual hydrazine-reduced graphene oxide sheets,[44] with the most probable mechanism for charge migration being variable-range-hopping and conduction being space-charge-limited.[45,46] Unfortunately, we cannot distinguish if our CARGO samples are n- or p-type semiconductors, since such measurements require instrumentation that is not suitable for our paper samples; however, we do not anticipate n-type conductivity due to the relatively low C/O ratios of these samples.

In conjunction with good electrical conductivity, the presence of functional groups on the CARGO surface may improve their performance beyond that of graphene in a variety of applications including charge storage and electrochemical sensing.[6] To this end, we functionalized the fabricated CARGO papers with hexylamine, as alkylamines have been found to intercalate into the intersheet gallery in GO[47] and to effect the covalent functionalization of graphene oxide paper *via* epoxide amination.[48] After hexylamine treatment, the mass of our CARGO paper samples prepared in DMF, DMSO, and NMP increased by 8.6, 9.4, and 5.9%, respectively. For comparison, the corresponding unreduced graphene oxide papers, prepared in the same solvents but without heating, exhibited an average increase of 13.5% (Table S2 in SI) after similar hexylamine treatments. The smaller values for mass gain in the CARGO samples again support the more reduced nature of these materials. Most importantly, the broad range of mass gain (from 6 to 13%) indicates that the surface chemistry of graphene oxide-based papers can be readily tuned simply by selecting the appropriate refluxing solvent during synthesis.

The successful functionalization of the CARGO surface by hexylamine was further confirmed *via* XRD, where all treated papers exhibited a new diffraction peak at ∼9.5 Å (Figure 6 and Figure S6 in SI). These peaks can only arise due to the incorporation of amine into the gallery spacing, which must expand to accommodate the new functional groups.[39,47,48] As the CARGO paper samples were extensively washed after amine treatment, these new functional groups are most likely chemisorbed to the surface of the CARGO nanosheets (see also discussion of XPS and FT-IR data

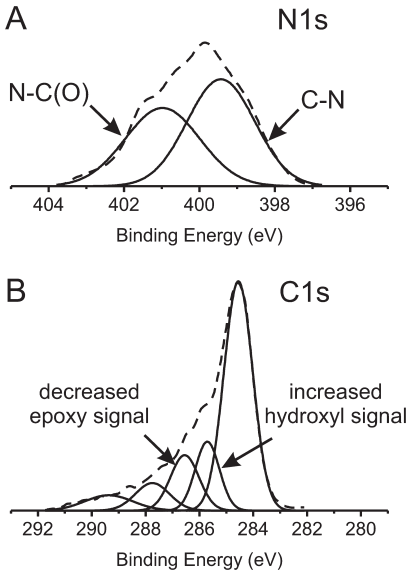

Figure 7. XPS spectra of the N1s (A) and C1s (B) regions of hexylamine-modified CARGO. The ratio between signals from hydroxyl (∼285.6 eV) and epoxy (∼286.7 eV) groups has increased in comparison to that observed for an unmodified sample (see Figure 4D).

below), as has been previously established in graphene oxide papers.[39,48] The presence of two diffraction peaks is not unexpected, as hexylamine-functionalized graphene paper has been previously observed to exhibit peaks for both closely packed graphene layers (3.94 Å) and amine-separated layers (8.14 Å).[39]

Spectral characterization of the amine-functionalized CARGO samples prepared in DMF and NMP is complicated by the presence of C−N bonds in residual solvents. As such, the chemical nature of the post-functionalization CARGO paper could only be unequivocally established for the sample prepared *via* DMSO reflux. XPS analysis of the N1s region (Figure 7A) of the amine-treated, DMSO-prepared CARGO sample confirms the presence of N atoms, while the C1s region (Figure 7B) reveals a *decrease* in signal intensity from the *epoxy* groups and a corresponding *increase* in signal intensity from the *hydroxyl* groups on the amine-treated CARGO surface. These changes correspond well with a previously proposed scheme for amine functionalization of graphene oxide *via* epoxide amination.[39] Further supporting this observation is the presence of a broad stretch for ν(C−N) near 1130 cm^{-1} in the FT-IR spectrum of the amine-treated CARGO sample (Figure 5). The formation of additional thermally labile hydroxyl groups[41] during epoxide amination may offer a means to further reduce DMSO-prepared CARGO samples after amine treatment, as the hydroxyl groups should be readily removed with additional heating near 150 °C, while covalently bound alkylamines require temperatures near 250 °C to initiate their desorption.[39]

Tuning the CARGO Surface *via* Chemical Functionalization. While we have clearly demonstrated that the C/O ratio of CARGO can be readily tuned by varying reflux temperature (see Table 1 and the accompanying discussion above), the aforementioned hexylamine-functionalization experiments suggest that our three CARGO samples do not react with hexylamine in a fashion that correlates simply to the C/O ratio. Thus, it is possible that the thermal treatment of graphene oxide in different solvents would result in new types of nanosheet materials possessing different distributions of functional groups. To this end, we attempted to tune the density of the specific functional groups on the CARGO sheets using organic amines and isocyanates.

Amines readily ring-open the surface-bound epoxide groups of graphene oxide,[39,49] which remain in relative abundance after reflux in DMF and DMSO, but not in NMP, as determined by XPS and FT-IR spectra (see Characterization of CARGO Papers section above). Indeed, after treatment of CARGO with 4-chlorobenzylamine in solution, C/amine ratios of 67, 59, and 156 were achieved in samples prepared in DMF, DMSO, and NMP, respectively (Table 2, also see SI for sample calculations from EA data). As expected from the moderately high C/O ratios of our CARGO samples, these ratios are higher than those observed for 4-chlorobenzylamine-treated unreduced graphene oxide, where a C/amine ratio of 18 was observed, in line with ratios determined for alkylamine-treated graphene oxide papers.[39,48] We note that the level of amine functionalization decreases nearly 3-fold in going from the CARGO prepared in DMF and DMSO to that prepared in NMP, which is in good agreement with the lower epoxide concentration on the NMP-refluxed nanosheets in comparison to the relatively high epoxide density on the other two CARGO samples that were prepared at lower temperatures (see Characterization of CARGO Papers section above). That such a wide range of C/amine ratios can be achieved from unreduced graphene oxide to NMP-prepared CARGO suggests good control over the degree of amine functionalization, with the possibility for fine-tuning if CARGO is prepared from solvents with intermediate boiling points.

Orthogonal to the epoxide amination, organic isocyanates have been found to preferentially react with hydroxyl groups on the CARGO surface *via* nucleophilic addition[50] and carboxyl groups at the edge of the nanosheets *via* condensation[51] reactions to afford carbamate and amide groups, respectively. As hydroxyl and carboxyl groups were largely reduced *via* our thermal treatment (see Characterization of CARGO Papers section above), reaction with isocyanates should not occur to any great extent in CARGO. We were pleased to observe that reaction of CARGO with 4-chlorophenyl isocyanate reveals C/isocyanate ratios of 130, 273, and 349 for samples prepared in DMF, DMSO, and NMP, respectively. These ratios are higher than the ratios observed in the aforementioned 4-chlorobenzylamine functionalizations and much higher than that observed for the isocyanate functionalizations of unreduced graphene oxide (C/isocyanate ratio = 19). We note that the C/isocyanate ratios increase linearly with the C/O ratio, which corresponds well with recent theoretical simulations[41] that predict increasing loss of hydroxyl groups from graphene oxide with increasingly higher temperature. This suggests that the C/O ratio can serve as an excellent control for the degree of isocyanate functionalization, as a linear relationship also exists between this ratio and the boiling point of the solvent from which the CARGO is prepared.

TABLE 2. The Amine- and Isocyanate-Functionalization of CARGO Samples Prepared by Refluxing Graphene Oxide in DMF, DMSO, and NMP. Data for Unreduced Graphene Oxide Are Included for Comparison

	amine functionalization		isocyanate functionalization	
refluxing solvent	C/O ratio	C/amine ratio[a]	C/O ratio	C/isocyanate ratio[a]
no reflux (*i.e.*, unreduced)	1.6	17.6	1.6	19.1
DMF	2.7	66.7	2.8	130.2
DMSO	3.9	58.7	4.0	273.5
NMP	4.2	156.0	4.3	349.4

[a] See SI for sample calculations of C/amine and C/isocyanate ratios.

Functionalized CARGO as a Lithium-Ion Battery Anode with Improved Capacities. As mentioned in the introduction, graphene paper has been utilized as a binder-free electrode material in lithium ion batteries.[7,8] However, the primary limitation in the performance of graphene paper anodes is significant irreversible capacity during the initial charge/discharge cycle where Coulombic efficiencies (the % ratio of charge to discharge capacity) as low as 12.4% have been reported.[7] Such poor reversibility can be attributed to the formation of a solid-electrolyte interface (SEI) on the paper surface,[8] which stabilizes the battery during charge and discharge at the expense of battery performance. In a Li/graphite half cell, SEI formation occurs at low voltage *via* the decomposition of electrolyte molecules (*e.g.*, cyclic and linear alkyl carbonates) during the initial lithiation.[52] In tightly packed structures like graphite, where electrolyte molecules are not easily dispersed throughout the inter sheet gallery, this process occurs in an ill-defined manner, resulting in low reversible capacity.[53] We hypothesize that in functionalized CARGO paper anodes, where the functional groups on the basal plane may provide slightly increased intersheet spacing (Figure S9 in SI) and nucleation sites, the SEI formation would be facilitated and better controlled, leading to higher reversible capacity. To this end, we tested 4-chlorophenyl isocyanate-treated CARGO, which features carbamate and linkages on the basal plane that

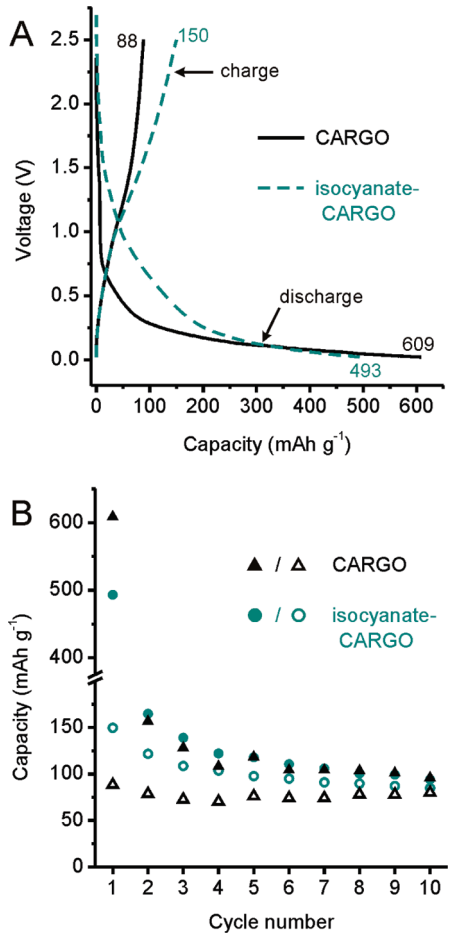

Figure 8. (A) Initial charge/discharge profiles for binder-free anode papers fabricated from CARGO and 4-chlorophenyl isocyanate-functionalized CARGO. (B) Cycling performance of CARGO (triangles) and functionalized CARGO (circles) anodes. Charge and discharge values are denoted by empty and solid shapes, respectively. All data were collected at a current rate of 20 mA g^{-1}.

can interact well with carbonate-based electrolytes as well as lithium ions, as an anode in a lithium cell.

4-Chlorophenyl isocyanate-treated CARGO prepared from DMF was used to maximize coverage of the functional groups, as this sample contains the lowest C/isocyanate ratio (Table 2). The presence of these groups raises the sheet resistance of the treated sample to 37 kΩ per square from a value of only 7 kΩ per square for untreated CARGO. The decreased ability of electrons to flow through CARGO after functionalization may contribute to the improved performance of the SEI layer, where poor electrical conductivity must be coupled with good ionic conductivity to maximize lithium ion transport in lieu of recombination. Neat and functionalized CARGO both exhibit charge/discharge profiles similar to that of disordered carbon (Figure 8A),[54] which can be attributed to their exfoliated nature and the presence of oxygen-containing moieties on the nanosheet surface. During the initial charge/discharge cycle, the isocyanate-functionalized paper electrode exhibits a Coulombic efficiency of 30% (Figure 8B), *over twice that of non-functionalized CARGO paper* (14%). Additionally, the initial reversible capacity of the treated paper (150 mAh g^{-1} at 20 mA g^{-1} current density) rivals that of hydrazine-reduced graphene paper,[8] which has a much higher C/O ratio of 5, and is *70% higher than that of the non-functionalized CARGO sample* (88 mAh g^{-1} at 20 mA g^{-1} current density). That such improvements resulted from isocyanate functionalization further emphasizes the potential broad utility of CARGO, where chemical functionalization can be utilized as a route to improving myriad properties above those of the parent nanosheet.

CONCLUSION

We have demonstrated that dispersions of electrically conductive, chemically active reduced graphene oxide (CARGO) can be readily prepared by refluxing graphene oxide for a short time in the appropriate organic solvents. The C/O ratio of CARGO after heat treatment can be modulated according to the boiling point of the solvent, allowing for the functional group composition of CARGO nanosheets to be tuned in a well-controlled fashion. Hydroxyl and carboxyl groups are readily removed in thermal treatments above 155 °C, while epoxides are more resilient, being removable only when the temperature is higher than 200 °C, as in the case of NMP reflux. This facile thermal-tuning of the C/O ratios of CARGO allows us to control the dispersion of these nanosheets within a hydrophobic polystyrene matrix as well as the optical transparency of the resulting CARGO-polystyrene nanocomposite. CARGO with low C/O ratios formed nanocomposites that are lighter in color and contain large aggregates of the nanosheets, while those with higher C/O ratios afforded nanocomposites that are more opaque with excellent dispersion of the nanofiller.

As prepared, CARGO nanosheets comprise a class of materials with hybrid properties: they have electrical conductivity at least 5 orders of magnitude larger than that of graphene oxide (Table 1) while still retaining the chemical reactivity of graphene oxide in reactions with organic amines and isocyanates. CARGO can be fabricated into flexible papers that are both electrically conductive and reactive toward hexylamine, whose loadings can be varied according to C/O ratio: the more reduced samples prepared in NMP incorporate less amine than more oxidized samples prepared in DMF. A benefit of functionalizing CARGO was demonstrated by its use in the fabrication of lithium ion battery anodes. A CARGO-based anode treated with 4-chlorophenyl isocyanate exhibited much higher Coulombic efficiency and reversible capacity than one left untreated. This suggests that functionalized CARGO may be employed to improve the performance of devices that require both electrical conductivity and chemical activity. For example,

CARGO thin films could serve as highly selective and sensitive gas sensors,[6] where selectivity could be enhanced *via* surface functionalization and conductivity would provide a means for signal transduction. The ability to selectively tune the coverage of specific functional groups on the CARGO surface bestows a wide combination of properties to these nanosheets so they can be used in a large array of applications including those that demand high functional group density (*e.g.*, as a drug delivery template[55]) or others that require sparse distribution of groups (*e.g.*, transparent conductive thin films).[26]

EXPERIMENTAL SECTION

Materials. SP-1 graphite powder was used as received from Bay Carbon, Inc. (Bay City, MI). Hydrazine monohydrate (98%, 65 wt % N_2H_4) was obtained from Alfa Aesar, Inc. (Ward Hill, MA) and stored under a blanket of N_2 to discourage oxidation. 4-Chlorobenzylamine (97%+) and 4-chlorophenyl isocyanate (98%) were obtained from Alfa Aesar, Inc. and stored in a N_2-filled glovebox. *N*,*N*-dimethylformamide (DMF, 99.8%), dimethylsulfoxide (DMSO, 99.9%), and *N*-methylpyrrolidone (NMP, 99.8%) were used as received from Aldrich Chemicals, Inc. (Milwaukee, WI). Anhydrous DMSO was obtained from a Dow-Grubbs solvent system installed by Glass Contours, Inc. (now SG Waters USA (Nashua, NH)). Ultrapure deionized water (resistivity >18 MΩ cm) was obtained from a Milli-Q Biocel system.

Anodisc membranes (0.2 μm pore size, 47 mm diameter) from Whatman PLC (Maidstone, Kent, UK) were used during filtration for support of fabricated papers. Spectra/Por Membrane 6−8 kD molecular weight cutoff (MWCO) dialysis tubing was utilized to remove excess ions from solution. Molecular sieves (M-9882, 3 Å pore diameter) were received from Sigma (St. Louis, MO) and activated by heating at 500 °C for 6 h, cooled down to 100 °C, and stored in a glovebox prior to their use in drying organic dispersions of graphene oxide and CARGO. Sonication was performed using a VC505 Vibra-cell probe sonicator (500 W) equipped with a solid titanium−aluminum−vanadium tip (Sonics & Materials, Inc., Newton, CT). An Eppendorf model 5804 R centrifuge was employed for centrifugation.

Preparation of Graphene Oxide Dispersions. Graphite oxide (GO) was prepared using a modified Hummers procedure (see SI for synthetic details).[56−58] An aqueous graphene oxide dispersion was prepared according to a literature protocol[24] by suspending the synthesized GO in water and sonicating for 30 min (30% amplitude, 10 s pulses alternating with 10 s rest periods). This dispersion was purified *via* centrifugation and dialysis (see SI for purification details). Complete exfoliation of GO into graphene oxide in the dispersion was confirmed by the absence of a diffraction peak in the X-ray diffraction (XRD) pattern of a freeze-dried aliquot.

Synthesis of Colloidal CARGO *via* Thermal Treatment. Preparation of CARGO dispersions was achieved by diluting an aqueous dispersion (8.5 mg mL^{-1}) of graphene oxide (30 mg graphene oxide content), to a concentration of 0.5 mg mL^{-1} in either DMF, DMSO, or NMP.[9] Thermal reduction was carried out by either heating each dispersion at a specified temperature or refluxing at the boiling point of the solvent, for either 1 or 12 h with continuous mechanical stirring. Any flocculate observed in the sample after reduction was redispersed by sonication for 30 s (30% amplitude, 10 s pulses alternating with 10 s rest periods).

Fabrication of Nanocomposites. Polystyrene-based nanocomposites were prepared by dissolving polystyrene (693 mg) in DMF (100 mL), to which a dispersion of CARGO (7 mg, enough to make a 1 wt % nanocomposite) in its appropriate solvent, was added dropwise. When CARGO samples prepared in DMF and NMP were added to the polystyrene solution, this protocol afforded homogeneous composite solutions, which were subsequently precipitated in methanol (250 mL). When the CARGO sample prepared in DMSO was added to the polystyrene solution, a precipitate immediately formed so methanol precipitation was not needed. All precipitates were then isolated from solution by filtration and washed thoroughly with methanol (3 × 50 mL). The isolated powder samples were dried overnight in a vacuum oven at 80 °C before being hot-pressed into ∼0.25 mm thick films following a previously outlined procedure (see SI for details).[37] The 0.025 wt % nanocomposites were prepared in a similar manner from a solution of polystyrene (4 g) in DMF (500 mL) and a dispersion of CARGO (1 mg, enough to make a 0.025 wt % nanocomposite).

Fabrication of papers. Self-supporting CARGO and graphene oxide papers were prepared by filtering the appropriate dispersion, through an Anodisc filter membrane under vacuum assistance.[4,59] A Kontes Ultraware microfiltration apparatus equipped with a fritted glass support base was utilized for filtration. Fabricated papers were dried in air before removal from the filter membrane for further treatment and characterization. As our paper samples were fully dried in air to remove all residual solvent prior to data collection, solvent-swelling is not a major concern in our study.

Functionalization of Graphene Oxide and CARGO with 4-Chlorobenzylamine or 4-Chlorophenyl Isocyanate. Dispersions of graphene oxide and CARGO in DMF, DMSO, and NMP (30 mL, 0.5 mg mL^{-1}) were transferred to a glovebox and dried for 24 h over activated molecular sieves (3 Å pore diameter) to remove any residual water from the original aqueous dispersion. These dispersions were then transferred to round-bottom flasks containing either 4-chlorobenzylamine (0.25 mmol) or 4-chlorophenyl isocyanate (0.25 mmol). The resulting mixtures were stirred for 18 h before being removed from the glovebox. The dispersions of functionalized graphene oxide and CARGO were then fabricated into papers as described above and washed by soaking for 24 h in the respective solvent (50 mL), whose volume was replaced every 6 h.

Functionalization of CARGO Paper with Hexylamine. Fabricated CARGO papers were soaked in 0.1 M solutions of hexylamine (50 mL, in the respective organic solvent from which each sample was prepared) for 24 h to allow for complete intercalation of the amine into the layered paper structure.[48] After reaction, the papers were subjected to four 6 h soaking cycles in the same solvent from which each sample was prepared to remove physisorbed amines. The samples were then dried in air overnight before characterization.

Characterization. Thermogravimetric analysis (TGA) was performed in the Polymer Characterization Laboratory at Northwestern University (NU) using a Mettler-Toledo TGA/SDTA851 analyzer (Columbus, OH) with samples heated in alumina crucibles from 50 to 800 °C in a N_2 atmosphere with a scanning rate of 10 °C min^{-1}. Elemental analysis (EA) was performed at Atlantic Microlabs (Norcross, GA). Scanning electron microscope (SEM) images were gathered in the NEMS-MEMS Facility at NU using a field-emission gun Nova NanoSEM 600 (FEI Co., Hillsboro, OR) microscope.

X-ray photoelectron spectroscopy (XPS) and Fourier-transform infrared spectroscopy (FT-IR) analyses were performed in the Keck II/NUANCE facility at NU. XPS data collection was performed with an Omicron (Taunusstein, Germany) ESCA Probe (Al Kα radiation, $h\nu$ = 1486.6 eV). A Shirley background was removed from atomic spectra prior to deconvolution. FT-IR spectra were collected in absorbance mode using a Thermo Nicolet (Waltham, MA) Nexus 870 FT-IR spectrometer. A linear baseline was removed from all spectra. XRD patterns were collected in the J. B. Cohen X-ray Diffraction Facility at NU with a Rigaku 2000 diffractometer (Rigaku, Inc., The Woodlands, TX) using nickel filtered Cu Kα radiation (λ = 1.5406 Å). A cubic spline background was removed from all reported patterns.

Electrical conductivity measurements were carried out on narrow strips of CARGO paper with dimensions of 2 × 10 × 0.01 mm (width × length × thickness). These strips were cut from larger pieces of the as-prepared paper by compression with a razor blade parallel to the edge of a microscope slide as a guide. In this manner the formation of stray cracks along the edges of the strip, which often occur with a sliding cut strategy, can be eliminated. Lateral dimensions were measured with a digital caliper and thickness was determined using SEM images (Figure S7 in SI). A colinear four-probe arrangement was used for all electrical measurements, and contact pads were prepared with a silver-filled conductive epoxy (McMaster-Carr, Robbinsville, NJ). A Keithley 6221 Current Source (Keithley, Inc., Cleveland, OH) was used for low current measurements, while higher current measurements were achieved using a direct current power supply (model 6544A, Agilent Technologies, Santa Clara, CA), and voltage was measured with a Keithley 6514 System Electrometer.

Charge−discharge profiles and cycle performance data for neat and functionalized CARGO paper were collected at Argonne National Laboratory in a CR 2032-type coin cell configuration using a Maccor battery cycler (Maccor, Inc., Tulsa, OK). Lithium metal foil served as the counter electrode and the electrolyte consisted of a mixture of ethylene carbonate and ethyl methyl carbonate (3:7 w/w) and lithium ions in the form of $LiPF_6$ (1.2 M). All samples were heated at 75 °C for 3 h to remove residual moisture before being transferred to a He-filled glovebox. Cells were charged and discharged at a current rate of 20 mA g^{-1}.

Acknowledgment. This work was supported by the NSF (Award No. DMR-0520513 through the Materials Research Science and Engineering Center at Northwestern University), ARO (Award No. W991NF-09-1-0541), and the U.S. Department of Energy (FreedomCar, Vehicle Technology Office). O.C.C. is an NSF-ACC fellow (Award No. CHE-0936924). Argonne National Laboratory is a U.S. Department of Energy Office of Science laboratory operated under Contract No. DE-AC02-06CH11357. We thank the Initiative for Sustainability and Energy (ISEN) at Northwestern for funding the purchase of some of the equipments used in this work. We are grateful to the reviewers of this manuscript for their suggestions, which greatly strengthen the final paper.

Supporting Information Available: Experimental details, characterization (XRD patterns and FT-IR spectra) of graphene oxide, and CARGO samples prepared from DMF and NMP, TGA profile of graphene oxide, and example calculations of C/functional group ratios from EA data. This material is available free of charge *via* the Internet at http://pubs.acs.org.

REFERENCES AND NOTES

1. Lee, C.; Wei, X.; Kysar, J. W.; Hone, J. Measurement of the Elastic Properties and Intrinsic Strength of Monolayer Graphene. *Science* **2008,** *321*, 385–388.
2. Balandin, A. A.; Ghosh, S.; Bao, W.; Calizo, I.; Teweldebrhan, D.; Miao, F.; Lau, C. N. Superior Thermal Conductivity of Single-Layer Graphene. *Nano Lett.* **2008,** *8*, 902–907.
3. Orlita, M.; Faugeras, C.; Plochocka, P.; Neugebauer, P.; Martinez, G.; Maude, D. K.; Barra, A. L.; Sprinkle, M.; Berger, C.; de Heer, W. A.; *et al.* Approaching the Dirac Point in High-Mobility Multilayer Epitaxial Graphene. *Phys. Rev. Lett.* **2008,** *101*, 267601/1–4.
4. Chen, H.; Muller, M. B.; Gilmore, K. J.; Wallace, G. G.; Li, D. Mechanically Strong, Electrically Conductive, and Biocompatible Graphene Paper. *Adv. Mater.* **2008,** *20*, 3557–3561.
5. Stankovich, S.; Dikin, D. A.; Dommett, G. H. B.; Kohlhaas, K. M.; Zimney, E. J.; Stach, E. A.; Piner, R. D.; Nguyen, S. T.; Ruoff, R. S. Graphene-Based Composite Materials. *Nature* **2006,** *442*, 282–286.
6. Fowler, J. D.; Allen, M. J.; Tung, V. C.; Yang, Y.; Kaner, R. B.; Weiller, B. H. Practical Chemical Sensors from Chemically Derived Graphene. *ACS Nano* **2009,** *3*, 301–306.
7. Wang, C.; Li, D.; Too, C. O.; Wallace, G. G. Electrochemical Properties of Graphene Paper Electrodes Used in Lithium Batteries. *Chem. Mater.* **2009,** *21*, 2604–2606.
8. Abouimrane, A.; Compton, O. C.; Amine, K.; Nguyen, S. T. Non-annealed Graphene Paper as a Binder-free Anode for Lithium-Ion Batteries. *J. Phys. Chem. C* **2010,** *114*, 12800–12804.
9. Park, S.; An, J. H.; Jung, I. W.; Piner, R. D.; An, S. J.; Li, X. S.; Velamakanni, A.; Ruoff, R. S. Colloidal Suspensions of Highly Reduced Graphene Oxide in a Wide Variety of Organic Solvents. *Nano Lett.* **2009,** *9*, 1593–1597.
10. Park, S.; Ruoff, R. S. Chemical Methods for the Production of Graphenes. *Nat. Nanotechnol.* **2009,** *4*, 217–224.
11. Lerf, A.; He, H.; Forster, M.; Klinowski, J. Structure of Graphite Oxide Revisited. *J. Phys. Chem. B* **1998,** *102*, 4477–4482.
12. Szabo, T.; Berkesi, O.; Dekany, I. Drift Study of Deuterium-Exchanged Graphite Oxide. *Carbon* **2005,** *43*, 3186–3189.
13. Cai, W. W.; Piner, R. D.; Stadermann, F. J.; Park, S.; Shaibat, M. A.; Ishii, Y.; Yang, D. X.; Velamakanni, A.; An, S. J.; Stoller, M.; *et al.* Synthesis and Solid-State NMR Structural Characterization of ^{13}C-Labeled Graphite Oxide. *Science* **2008,** *321*, 1815–1817.
14. Szabo, T.; Berkesi, O.; Forgo, P.; Josepovits, K.; Sanakis, Y.; Petridis, D.; Dekany, I. Evolution of Surface Functional Groups in a Series of Progressively Oxidized Graphite Oxides. *Chem. Mater.* **2006,** *18*, 2740–2749.
15. Compton, O. C.; Nguyen, S. T. Graphene Oxide, Highly Reduced Graphene Oxide, and Graphene: Versatile Building Blocks for Carbon-Based Materials. *Small* **2010,** *6*, 711–723.
16. Stankovich, S.; Piner, R. D.; Nguyen, S. T.; Ruoff, R. S. Synthesis and Exfoliation of Isocyanate-Treated Graphene Oxide Nanoplatelets. *Carbon* **2006,** *44*, 3342–3347.
17. Niyogi, S.; Bekyarova, E.; Itkis, M. E.; McWilliams, J. L.; Hamon, M. A.; Haddon, R. C. Solution Properties of Graphite and Graphene. *J. Am. Chem. Soc.* **2006,** *128*, 7720–7721.
18. Stoller, M. D.; Park, S.; Zhu, Y.; An, J.; Ruoff, R. S. Graphene-Based Ultracapacitors. *Nano Lett.* **2008,** *8*, 3498–3502.
19. Zhang, J.; Zhang, F.; Yang, H.; Huang, X.; Liu, H.; Zhang, J.; Guo, S. Graphene Oxide as a Matrix for Enzyme Immobilization. *Langmuir* **2010,** *26*, 6083–6085.
20. Patil, A. J.; Vickery, J. L.; Scott, T. B.; Mann, S. Aqueous Stabilization and Self-Assembly of Graphene Sheets into Layered Bio-nanocomposites Using DNA. *Adv. Mater.* **2009,** *21*, 3159–3164.
21. Schniepp, H. C.; Li, J. L.; McAllister, M. J.; Sai, H.; Herrera-Alonso, M.; Adamson, D. H.; Prud'homme, R. K.; Car, R.; Saville, D. A.; Aksay, I. A. Functionalized Single Graphene Sheets Derived from Splitting Graphite Oxide. *J. Phys. Chem. B* **2006,** *110*, 8535–8539.
22. McAllister, M. J.; Li, J. L.; Adamson, D. H.; Schniepp, H. C.; Abdala, A. A.; Liu, J.; Herrera-Alonso, M.; Milius, D. L.; Car, R.; Prud'homme, R. K.; *et al.* Single Sheet Functionalized Graphene by Oxidation and Thermal Expansion of Graphite. *Chem. Mater.* **2007,** *19*, 4396–4404.
23. Li, D.; Muller, M. B.; Gilje, S.; Kaner, R. B.; Wallace, G. G. Processable Aqueous Dispersions of Graphene Nanosheets. *Nat. Nanotechnol.* **2008,** *3*, 101–105.
24. Stankovich, S.; Dikin, D. A.; Piner, R. D.; Kohlhaas, K. A.; Kleinhammes, A.; Jia, Y.; Wu, Y.; Nguyen, S. T.; Ruoff, R. S. Synthesis of Graphene-Based Nanosheets *via* Chemical Reduction of Exfoliated Graphite Oxide. *Carbon* **2007,** *45*, 1558–1565.
25. Gao, W.; Alemany, L. B.; Ci, L.; Ajayan, P. M. New Insights into the Structure and Reduction of Graphite Oxide. *Nat. Chem.* **2009,** *1*, 403–408.
26. Fernández-Merino, M. J.; Guardia, L.; Paredes, J. I.; Villar-Rodil, S.; Solís-Fernández, P.; Martínez-Alonso, A.; Tascón, J. M. D. Vitamin C is an Ideal Substitute for Hydrazine in the Reduction of Graphene Oxide Suspensions. *J. Phys. Chem. C* **2010,** *114*, 6426–6432.
27. Stankovich, S.; Piner, R. D.; Chen, X. Q.; Wu, N. Q.; Nguyen, S. T.; Ruoff, R. S. Stable Aqueous Dispersions of Graphitic Nanoplatelets *via* the Reduction of Exfoliated Graphite Oxide in the Presence of Poly(sodium 4-styrenesulfonate). *J. Mater. Chem.* **2006,** *16*, 155–158.

28. Gao, J.; Liu, F.; Liu, Y.; Ma, N.; Wang, Z.; Zhang, X. Environment-Friendly Method to Produce Graphene That Employs Vitamin C and Amino Acid. *Chem. Mater.* **2010,** *22*, 2213–2218.
29. Villar-Rodil, S.; Paredes, J. I.; Martinez-Alonso, A.; Tascon, J. M. D. Preparation of Graphene Dispersions and Graphene-Polymer Composites in Organic Media. *J. Mater. Chem.* **2009,** *19*, 3591–3593.
30. Zhu, Y.; Stoller, M. D.; Cai, W.; Velamakanni, A.; Piner, R. D.; Chen, D.; Ruoff, R. S. Exfoliation of Graphite Oxide in Propylene Carbonate and Thermal Reduction of the Resulting Graphene Oxide Platelets. *ACS Nano* **2010,** *4*, 1227–1233.
31. Jeong, H.-K.; Lee, Y. P.; Jin, M. H.; Kim, E. S.; Bae, J. J.; Lee, Y. H. Thermal Stability of Graphite Oxide. *Chem. Phys. Lett.* **2009,** *470*, 255–258.
32. Wang, H. L.; Robinson, J. T.; Li, X. L.; Dai, H. J. Solvothermal Reduction of Chemically Exfoliated Graphene Sheets. *J. Am. Chem. Soc.* **2009,** *131*, 9910–9911.
33. Dubin, S.; Gilje, S.; Wang, K.; Tung, V. C.; Cha, K.; Hall, A. S.; Farrar, J.; Varshneya, R.; Yang, Y.; Kaner, R. B. A One-Step, Solvothermal Reduction Method for Producing Reduced Graphene Oxide Dispersions in Organic Solvents. *ACS Nano* **2010,** *4*, 3845–3852.
34. Gao, X.; Jang, J.; Nagase, S. Hydrazine and Thermal Reduction of Graphene Oxide: Reaction Mechanisms, Product Structures, and Reaction Design. *J. Phys. Chem. C* **2009,** *114*, 832–842.
35. We note with interest that the exact opposite of this trend has been observed for graphene oxide heated at 150 and 200 °C in propylene carbonate.
36. Lin, Z.; Yao, Y.; Li, Z.; Liu, Y.; Li, Z.; Wong, C.-P. Solvent-Assisted Thermal Reduction of Graphite Oxide. *J. Phys. Chem. C* **2010,** *114*, 14819–14825.
37. Compton, O. C.; Kim, S.; Pierre, C.; Torkelson, J. M.; Nguyen, S. T. Crumpled Graphene Nanosheets as Highly Effective Barrier Property Enhancers. *Adv. Mater.* **2010,** *22*, 4759–4763.
38. Unfortunately, further drying of the CARGO paper samples by annealing could not be carried out due to the ease in which the paper can undergo further thermal reduction.
39. Compton, O. C.; Dikin, D. A.; Putz, K. W.; Brinson, L. C.; Nguyen, S. T. Electrically Conductive "Alkylated" Graphene Paper *via* Chemical Reduction of Amine-Functionalized Graphene Oxide Paper. *Adv. Mater.* **2010,** *22*, 892–896.
40. Konno, H.; Yamamoto, Y. Ylide-Metal Complexes .XIII: An X-ray Photoelectron Spectroscopic Study of Bis-(dimethylsulfoxonium methylide)Gold Chloride. *Bull. Chem. Soc. Jpn.* **1987,** *60*, 2561–2564.
41. Bagri, A.; Mattevi, C.; Acik, M.; Chabal, Y. J.; Chhowalla, M.; Shenoy, V. B. Structural Evolution During the Reduction of Chemically Derived Graphene Oxide. *Nat. Chem.* **2010,** *2*, 581–587.
42. We note that GO has been observed to retain most of the epoxides on its surface after dry annealing at 200 °C for 6 h.
43. Ruiz, J. C.; Macewan, D. M. C. Interlamellar Sorption Complexes of Graphitic Acid with Organic Substances. *Nature* **1955,** *176*, 1222–1223.
44. Gilje, S.; Han, S.; Wang, M.; Wang, K. L.; Kaner, R. B. A Chemical Route to Graphene for Device Applications. *Nano Lett.* **2007,** *7*, 3394–3398.
45. Jung, I.; Dikin, D. A.; Piner, R. D.; Ruoff, R. S. Tunable Electrical Conductivity of Individual Graphene Oxide Sheets Reduced At "Low" Temperatures. *Nano Lett.* **2008,** *8*, 4283–4287.
46. Joung, D.; Chunder, A.; Zhai, L.; Khondaker, S. I. Space Charge Limited Conduction with Exponential Trap Distribution in Reduced Graphene Oxide Sheets. *Appl. Phys. Lett.* **2010,** *97*, 093105/1–3.
47. Dekany, I.; Kruger-Grasser, R.; Weiss, A. Selective Liquid Sorption Properties of Hydrophobized Graphite Oxide Nanostructures. *Colloid Polym. Sci.* **1998,** *276*, 570–576.
48. Stankovich, S.; Dikin, D. A.; Compton, O. C.; Dommett, G. H. B.; Nguyen, S. T.; Ruoff, R. S. Systematic Post-Assembly Modification of Graphene Oxide Paper with Primary Alkylamines. *Chem. Mater.* **2010,** *22*, 4153–4157.
49. Bourlinos, A. B.; Gournis, D.; Petridis, D.; Szabo, T.; Szeri, A.; Dekany, I. Graphite Oxide: Chemical Reduction to Graphite and Surface Modification with Primary Aliphatic Amines and Amino Acids. *Langmuir* **2003,** *19*, 6050–6055.
50. Draye, A.; Tarasov, D.; Tondeur, J. Solvent-Assisted Alcohol-Isocyanate Kinetics. *React. Kinet. Catal. Lett.* **1999,** *66*, 199–204.
51. Blagbrough, I. S.; Mackenzie, N. E.; Ortiz, C.; Scott, A. I. The Condensation Reaction between Isocyanates and Carboxylic Acids. A Practical Synthesis of Substituted Amides and Anilides. *Tetrahedron Lett.* **1986,** *27*, 1251–1254.
52. Tarascon, J. M.; Armand, M. Issues and Challenges Facing Rechargeable Lithium Batteries. *Nature* **2001,** *414*, 359–367.
53. Andersson, A. M.; Edström, K. Chemical Composition and Morphology of the Elevated Temperature SEI on Graphite. *J. Electrochem. Soc.* **2001,** *148*, A1100–A1109.
54. Yoo, E.; Kim, J.; Hosono, E.; Zhou, H.-s.; Kudo, T.; Honma, I. Large Reversible Li Storage of Graphene Nanosheet Families for Use in Rechargeable Lithium Ion Batteries. *Nano Lett.* **2008,** *8*, 2277–2282.
55. Liu, Z.; Robinson, J. T.; Sun, X. M.; Dai, H. J. Pegylated Nanographene Oxide for Delivery of Water-Insoluble Cancer Drugs. *J. Am. Chem. Soc.* **2008,** *130*, 10876–10877.
56. Hummers, W. S.; Offeman, R. E. Preparation of Graphitic Oxide. *J. Am. Chem. Soc.* **1958,** *80*, 1339–1339.
57. Kovtyukhova, N. I.; Ollivier, P. J.; Martin, B. R.; Mallouk, T. E.; Chizhik, S. A.; Buzaneva, E. V.; Gorchinskiy, A. D. Layer-by-Layer Assembly of Ultrathin Composite Films from Micron-Sized Graphite Oxide Sheets and Polycations. *Chem. Mater.* **1999,** *11*, 771–778.
58. Hirata, M.; Gotou, T.; Horiuchi, S.; Fujiwara, M.; Ohba, M. Thin-Film Particles of Graphite Oxide 1: High-Yield Synthesis and Flexibility of the Particles. *Carbon* **2004,** *42*, 2929–2937.
59. Dikin, D. A.; Stankovich, S.; Zimney, E. J.; Piner, R. D.; Dommett, G. H. B.; Evmenenko, G.; Nguyen, S. T.; Ruoff, R. S. Preparation and Characterization of Graphene Oxide Paper. *Nature* **2007,** *448*, 457–460.